A Comparison of Modal Electromagnetic Field Distributions in Analytical and Numerical Solutions

Miloš Davidović, Anđelija Ilić[1], Miodrag Tasić[2], Branislav Notaroš[3], Milan Ilić[4]

Abstract – **In this paper, a detailed comparison of modal electromagnetic field distribution in two canonical microwave cavities, obtained via analytical and recently introduced numerical approaches, is presented and discussed. While the analyzed problems, namely, those of a spherical cavity and a ridged cavity are relatively simple, they still provide valuable benchmarks for novel numerical methods, allowing for early estimates of accuracy, efficiency, and convergence properties of the method. Furthermore, study of field distributions may provide useful insights about strengths and weaknesses of the approximating vector spaces which are otherwise not possible.**

Keywords – **Microwave cavities, Higher order finite element method, B-spline solid modeling, Eigenfrequency, Eigenfield.**

I. INTRODUCTION

Error estimates are a very important part of any kind of analysis performed in a modern electromagnetic (EM) engineering practice, especially for widely accepted methods such as finite element method (FEM) [1]. These kinds of estimates are also needed for all novel methods, whose properties are not yet studied in detail. Modern computational EM is largely oriented toward higher order methods, excellent survey of which can be found in [2]. Unfortunately, higher order methods require much more involvement from practicing engineers. Therefore, success (or failure) of EM engineering projects will still often be strongly determined by proficiency of practicing engineers in adequate formulation of the problem, i.e., use of sufficient number of details during geometrical modeling and meshing, setting reasonable prescribed accuracy, and interpretation of obtained numerical results. These skills are best honed by performing FEM known problems, which present reasonable amount of difficulties encountered in practice (such as curved geometry, singular fields) but are not overwhelming. It is therefore desirable for any novel method, to be tested on well understood, but not trivial problems. With this in mind, the B-spline method for efficient analysis of three dimensional (3-D) microwave cavities, recently introduced in [3], was tested in terms of accuracy and efficiency. Testing of accuracy was taken beyond the usually performed eigenvalue test, and also includes testing of eigenfield solution. The analyzed method enables completely independent higher order modeling of both geometry and electromagnetic fields; the geometry modeling is done using trivariate B-splines (by exploiting their excellent approximation capabilities), while the field modeling is done using hierarchical higher order polynomial vector basis functions [4] (thus enabling very accurate and efficient approximation of fields). It is worth noting that while some other methods for geometry modeling may represent some forms of geometry more accurately (for example rational Bézier curves and non-uniform rational B-splines or NURBS [5], [6] can model conic sections exactly), they may also require specialized quadrature rules when used in numerical EM.

In this paper, we revisit the B-spline FEM modeling introduced in [3] and give additional insight in the convergence of the modal field solutions. Section II of the paper presents the B-spline modeling of solids in general as well as details of solid modeling of spherical and ridged cavity in particular. In Section III, the FEM field-expansion basis functions are described. In Section IV, numerical results are discussed including analysis of modal field distributions.

II. B-SPLINE SOLID MODELING

Presentation in this Section mainly follows [3] regarding general B-spline solid modeling, with additional details on analyzed examples of the spherical and the ridged cavity.

A. Univariate B-splines

Since solid modeling requires utilization of trivariate splines, and they are defined using univariate splines, some basic univariate splines definitions are in place. Note however, that while univariate spline definitions that will be given below are constructive in nature, i.e., they describe one possible algorithm for construction of splines, it is more advisable to implement more stable and efficient algorithms [7]. We use the following recurrent formula to define the B-spline functions:

Miloš Davidović is with the School of Electrical Engineering, University of Belgrade, 11120 Belgrade, Serbia (PhD student) and also with Laboratory for radiation measurements 100, Vinča Institute, University of Belgrade, 11001 Belgrade, Serbia, E-mail: davidovic@vinca.rs

[1]Anđelija Ilić is with the Innovation Center, School of Electrical Engineering, University of Belgrade 11120 Belgrade, Serbia E-mail: andjelijailic@ieee.org

[2]Miodrag Tasić is with the School of Electrical Engineering, University of Belgrade, 11120 Belgrade, Serbia E-mail: tasic@etf.rs

[3]Branislav Notaroš is with the Department of Electrical and Computer Engineering, Colorado State University, Fort Collins, CO 80523-1373 USA E-mail: notaros@colostate.edu

[4]Milan Ilić is with the School of Electrical Engineering, University of Belgrade, 11120 Belgrade, Serbia, and also with the Department of Electrical and Computer Engineering, Colorado State University, Fort Collins, CO 80523-1373 USA E-mail: milanilic@etf.rs

$$B_{i,1}(u)=1,\ u_i\le u\le u_{i+1}\ \text{ and }\ B_{i,1}(u)=0,\text{elsewhere},$$
$$B_{i,m}(u)=\frac{u-u_i}{u_{i+m-1}-u_i}B_{i,m-1}(u)+\frac{u_{i+m}-u}{u_{i+m}-u_{i+1}}B_{i+1,m-1}(u),\ m>1 \quad (1)$$

where $0\le i\le n$, $n>0$, and $U=(u_0,u_1,\ldots,u_{n+m})$ is a non-decreasing sequence of real numbers. U is called the knot vector of the corresponding spline family, and can be used to flexibly increase or decrease the number of splines and continuity of splines over knot vectors with multiplicities. Multiplicities, i.e., repetition of knots in knot vector, can lead to non-defined terms in Eq. (1), and if division by zero should occur when algorithm from Eq. (1) is followed, that term is replaced by zero. The function $B_{i,m}(u)$ is called the i-th B-spline of order m and degree $m-1$ with respect to the knot vector U. The following equations hold for a standard clamped uniform knot vector:

$$u_i=0,\ 0\le i\le m-1,\quad u_i=i-m+1,\ m\le i\le n,\quad \text{and}$$
$$u_i=n-m+2,\ n+1\le i\le n+m, \quad (2)$$

where the term "uniform" refers to uniform spacing between internal knots, and the term "clamped" is due to end knot multiplicities.

B. Trivariate Splines and Hexahedron Parametrization

Using previously defined univariate B-splines, we can define a parametric hexahedron introducing a mapping $\mathbf{r}:(u,v,w)\to(x,y,z)$, $(u,v,w)\in[-1,1]\times[-1,1]\times[-1,1]$ (cubical parent domain), such that it is interpolatory at the specified points of the global Cartesian space. To simplify the parameterization (without loss of generality) we employ the same order of B-splines ($m_u=m_v=m_w=m$) and the same knot vectors in all directions. A point within a hexahedron is thus defined by

$$\mathbf{r}(u,v,w)=\sum_{i,j,k=0}^{n} B_{i,m}(u)B_{j,m}(v)B_{k,m}(w)\,\mathbf{C}_{i,j,k}. \quad (3)$$

where $B_{i,m}, B_{j,m}, B_{k,m}$ are the splines over the same knot vector and $\mathbf{C}_{i,j,k}$ are the position vectors of the control points, found by solving the following system of equations:

$$\mathbf{r}_l=\sum_{i,j,k=0}^{n} B_{i,m}(u^l)B_{j,m}(v^l)B_{k,m}(w^l)\,\mathbf{C}_{i,j,k},\ l=1,\ldots,K, \quad (4)$$

where $K=(n+1)^3$, and with $\mathbf{r}_l$ and (u^l,v^l,w^l) being the (global) position-vectors of the interpolation points of the solid and their (local) parametric coordinates, respectively. Note that other parameterization formulations are also possible (but slightly less simple). For example, Eq. (4) can be modified to include various additional conditions, such as prescribed tangent at certain points, etc. The choice of interpolation points and a knot vector depends on the particular solid that needs to be parameterized, and will be presented next.

C. Solid Modeling of the Spherical and Ridged cavity

Spherical cavity can be modeled as a solid in a number of ways (even when restriction to B-spline solid modeling is made). Note however, that utilization of polynomial models (or piece-wise polynomial) models are preferred, since rational functions would require specialized quadrature algorithms. We opted for the method described in previous section, with the choice of parametric and Cartesian points given by a simple analytical mapping [3]. This way, it is possible to have tunable geometrical accuracy, which is very important, especially when doing pointwise comparisons of the field quantities. Two solid spline models were used for the cavity, a more "crude" model, having only 125 interpolation points ($n=4$), and geometrically refined model, having 1,000 interpolation points ($n=9$).

Fig. 1 shows the spline functions used in the first model of the spherical cavity and parametric coordinate lines in the w=0 cut.

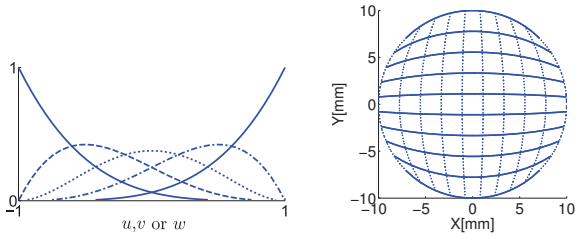

(a) (b)

Fig. 1. (a) B-spline functions of order m = 5 used for the entire-domain modeling of a spherical cavity with the flat knot vector $(-1,1)$ and (b) u-v coordinate lines in the w=0 cut

Note that both models are very precise and that visual inspection would not reveal any difference between the two. However, as we will show, eigenfield calculations are very sensitive and will reveal considerable differences between the two models.

Geometrical modeling of the ridged cavity is significantly simpler, partly because the cavity is swept geometry. Since, for simplicity, we use the same spline family in all three parametric directions, and 4 points are needed to describe the ridge, we will need a total of 4^3=64 interpolation points. Fig. 2 shows the interpolation points in one w-cut and the spline family used in all three parametric directions.

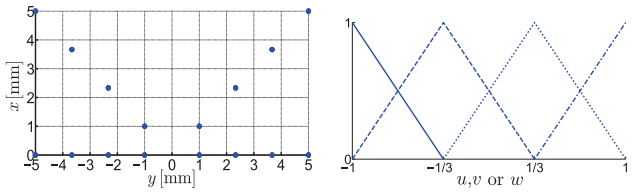

(a) (b)

Fig. 2. (a) Interpolation points in one w-cut and (b) B-spline family adopted for parameterization of the ridged cavity

These two examples clearly show flexibility of B-spline modeling, as both arbitrary order and arbitrary number of functions can be used along a parametric direction.

III. Field Expansion

Approximation of electric field is given (within each hexahedral element) as:

$$\mathbf{E}^e = \sum_{l=1}^{N^e} \gamma_l^e \, \mathbf{f}_l^e \tag{5}$$

where $\mathbf{f}_l^e$ are higher order vector basis functions with a total of N^e unknown field-distribution coefficients γ_l^e in the element. The basis functions are curl-conforming hierarchical polynomials of arbitrary field-approximation orders N_u^e, N_v^e, and N_w^e ($N_u^e, N_v^e, N_w^e \geq 1$) in the *e*-th element, which, for the reciprocal *u*-directed field vector, are given by:

$$\begin{aligned}
\mathbf{f}_{uqst}^e &= u^q P_s(v) P_t(w) \frac{\mathbf{a}_v^e \times \mathbf{a}_w^e}{\Im^e}, \\
P_s(v) &= \begin{cases} 1-v, & s=0 \\ v+1, & s=1 \\ v^s-1, & s \geq 2, \, even \\ v^s-v, & s \geq 3, \, odd \end{cases}, \\
\Im^e &= (\mathbf{a}_u^e \times \mathbf{a}_v^e) \cdot \mathbf{a}_w^e, \, \mathbf{a}_u^e = \frac{\partial \mathbf{r}^e}{\partial u}, \, \mathbf{a}_v^e = \frac{\partial \mathbf{r}^e}{\partial v}, \, \mathbf{a}_w^e = \frac{\partial \mathbf{r}^e}{\partial w},
\end{aligned} \tag{6}$$

where $\Im^e$ is the Jacobian of the covariant transformation, and $\mathbf{a}_u^e$, $\mathbf{a}_v^e$, and $\mathbf{a}_w^e$ are the unitary vectors along the parametric coordinates of the element and analogously for the *v*- and *w*-directed basis functions.

Field-expansion orders N_u^e, N_v^e, N_w^e in Eq. (6) are entirely independent from each other, and can be combined independently for the best overall performance of the method. Furthermore, because the basis functions are hierarchical (each lower-order set of functions is a subset of all higher-order sets), all of the parameters can be adopted anisotropically in different directions within an element, and nonuniformly from element to element in a model. Note that indices from Eq. (6) are "collapsed" into one index in Eq. (5). This scheme is commonly used when members of a set must be accessed in linear fashion. One well known example is from computer science when multidimensional arrays must be arranged in a linear sequence in memory.

It is interesting to note that basis functions defined by Eq.(6) can be classified into several different groups which play different role in FEM formulation. The first group consists of functions which have tangential component that vanishes on the element boundaries. In electric field approximation they do not directly participate in enforcement of boundary conditions. The *hp*-FEM literature commonly referes to these functions as the *bubble* functions. The second group consists of functions which have non vanishing tangential component on element boundaries, and are known as the *face* functions. These functions participate in approximation of boundary conditions. Note that with functions defined in Eq. (6) it is sufficient to enforce continuity of face functions, and no special algorithms need to be devised for edge, face, and vertex functions.

After Galerkin testing procedure, details of which can be found in [3], a generalized eigenvalue problem is obtained. Eigenvalues and eigenvectors (which come in form of coeeficients in Eq. (5)) are obtained as a solutions. Modal eigenfield is than easily obtained from Eq. (5).

IV. Numerical Results

For cavity problems, it is usually most important to obtain eigenfrequencies as accurately as possible. However, modal fields are also of interest. In the FEM algorithms the convergence is usually evaluated by comparison of S-parameters (for driven solutions), changes in overall scattering energy (for incident wave problems) or resonant frequencies (for eigenmode solutions) from pass to pass [8]. These quantities represent the results of the model as a whole, and usually converge more rapidly, i.e., with fewer unknowns, than the approximation of fields at individual points. However, it is interesting to study convergence of field solutions along with the convergence of eigenvalues, in order to gain better insight into needed number of unknowns, i.e., order of approximation, for specified accuracy. It is not uncommon for inexperienced engineers to set the prescribed accuracy too high, therefore considerably lengthening simulation times without any real benefit.

The electric field distribution for the dominant spherical mode obtained by the analytical solution [9] and by the entire domain B-spline solution, is given in Figs. 3 and 4, respectively. The field solutions are plotted directly from the computed corresponding eigenvectors, thus they are practically identical except for the difference in the eigenvector normalization (which is understandable) and except near the sphere "edges" (Fig. 4) where the entire-domain B-spline model has a discontinuous tangent (which is also easily appreciated and can be improved by adopting higher order geometrical model or *h*-refinement).

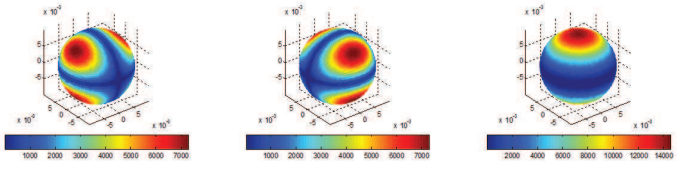

(a) (b) (c)

Fig. 3. Analytical solution: magnitudes of (a) *x*-, (b) *y*- and (c) *z*-components of the electric field for the first mode

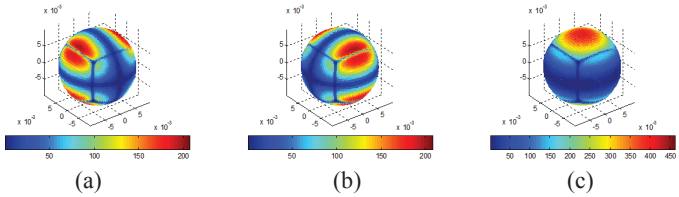

(a) (b) (c)

Fig. 4. B-spline solution (108 unknowns, "crude" geometry model): magnitudes of (a) *x*-, (b) *y*- and (c) *z*-components of the electric field for the first mode

Note that, in this case, any attempt to quantify the error of the field distribution throughout the element volume would be strongly biased by the significantly higher errors near these "edges".

However, to establish an estimate of the accuracy and convergence of the solution of the electric field, when the number of unknowns is increased (by *p*-refinement), we compute the RMS error of the magnitude of the B-spline field solution relative to the analytical solution for the two models of spherical cavity in 1,016 and 1,736 surface points for the crude and refined models, respectively. Numerical results for the RMS error of the dominant mode eigenfield for the two solid models, along with the average eigenfrequency error for the first 11 modes, are given in Table I.

Results from Table I can be interpreted in the following way. Looking at the convergence of the eigenfrequencies, it is clear that both models have excellent convergence, i.e., error decreases monotonically and rapidly with the increase of the number of unknowns. Situation is less clear regarding modal field convergence.

TABLE I
ERROR IN CALCULATING EIGENFREQUENCY AND MODAL FIELD IN A SPHERICAL CAVITY

	|Error| [%]			
	Average eigenfrequency error (11 modes)			
Crude model	2.8666	0.2011	0.1098	0.0501
Refined model	2.8179	0.1470	0.0661	0.0097
	RMS error in modal field (1st mode)			
Crude model	20.79	20.60	40.63	17.30
Refined model	10.29	9.70	5.11	5.08
Unknowns	108	240	450	756

It is evident that the error in modal field is several orders of magnitude larger than the error in eigenfrequencies. Also, with the refined model, the convergence is monotonic. On the other hand, the crude model shows high error despite excellent eigenvalue convergence. This can be attributed to the offset between the ideal spherical cavity used for exact analytical solution, and crude spline model of the sphere. Hence, there is effectively a significant mismatch of points when point-by-point comparison of fields is applied in presence of the rapidly changing fields (as can be seen from Figs. 3 and 4).

The ridged cavity (see [3] for more detailed figure of the cavity), is less grateful for comparison of modal field solutions because there is no readily available analytical solution. Hence, for the ridged cavity example, the B-spline solution and the reference numerical HFSS solution, for the dominant mode electric field distribution, are presented in the large number of sampling points in Fig. 5, where very similar distributions of fields can be observed. This is also confirmed by Fig. 6, where magnitude of the field is again plotted, but without 3D positional data, in order to include internal points in the comparison. Table II shows the relative error of the computed resonant free space wave number k_0 for the first 9 resonant modes.

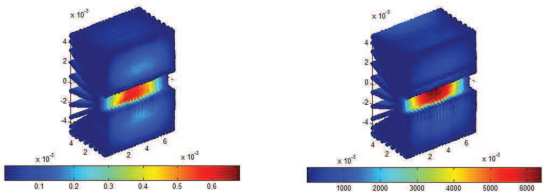

(a) (b)

Fig. 5. Magnitude of the electric field of the first mode of the ridge taken in the large number (27,000 points) of sampling points: (a) HFSS and (b) B-spline solutions

As for the modal field solution, RMS "error" for the first mode is 28.88%, when calculated in 27,000 volume points. This is again several orders of magnitude larger than the error in computed eigenfrequencies. This can be attributed to the fact that *p*-refined basis functions used in B-spline model are too smooth to model the field near reentrant corners of the ridge, where the field is theoretically singular. Furthermore, since there is no available exact solution, quantification of the error strongly depends on the HFSS solution (and its convergence properties, number of adaptive passes, and initial mesh seeding).

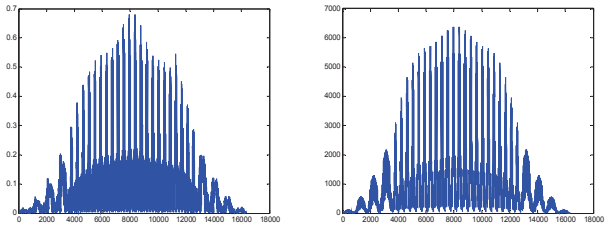

(a) (b)

Fig. 6. Plot of magnitude of the electric field of the first mode of the ridge, without 3D positional data, a) HFSS, b) B-spline

TABLE II
ERROR IN CALCULATING k_0 IN THE RIDGED CAVITY

Mode	HFSS k_0 [cm^{-1}]	B-spline |Error| [%]
Unknowns	3,017 t	276
1	5.091	0.0393
2	7.469	4.0969
3	7.853	0.4202
4	7.878	5.0774
5	8.019	3.8035
6	8.863	2.6853
7	8.9	4.3820
8	9.087	6.8119
9	10	3.9000

V. ACKNOWLEDGEMENTS

This work was supported by the Serbian Ministry of Education, Science, and Technological Development under grants ON171028 and TR-32005.

REFERENCES

[15] J. M. Jin, *The Finite Element Method in Electromagnetics*, 2nd ed., John Wiley & Sons, New York, 2002.
[16] B. M. Notaroš, "Higher order frequency-domain computational electromagnetics," *IEEE Trans. Antennas Propag.*, vol. 56, pp. 2251–2276, 2008.
[17] M. D. Davidović, B. M. Notaroš and M. M. Ilić, "B-spline entire-domain higher order finite elements for 3-D electromagnetic modeling," *IEEE Microwave and Wireless Components Letters*, vol. 22, no. 10, pp.497–499, 2012.
[18] M. M. Ilić, B. M. Notaroš, "Higher order hierarchical curved hexahedral vector finite elements for electromagnetic modeling," *IEEE Trans. Microw. Theory Techniques*, vol. 51, 1026–1033, 2003.
[19] L. Valle, F. Rivas and M. F. Cátedra, "Combining the moment method with geometrical modelling by NURBS surfaces and Bézier patches," *IEEE Trans. Antennas Propag.*, vol. 42, pp. 373–381, 1994.
[20] R. Coccioli, G. Pelosi and S. Selleri, "Optimization of bends in rectangular waveguide by a finite-element genetic-algorithm procedure," *Microw. Opt. Techn. Let.*, vol. 16, pp. 287–290, 1997.
[21] L. A. Piegl, W. Tiller, *The NURBs Book*, Springer-Verlag, 1997.
[22] HFSS ver. 11, Ansoft Corporation, Pittsburgh, PA, 2007.
[23] R. F. Harrington, *Time-Harmonic Electromagnetic Fields,* Wiley, 2001.